

# Optics Letters

## Interrogation of a linearly chirped fiber Bragg grating sensor with high resolution using a linearly chirped optical waveform

YIPING WANG,<sup>1,2</sup> JIEJUN ZHANG,<sup>1</sup> OLYMPIO COUTINHO,<sup>1</sup> AND JIANPING YAO<sup>1,\*</sup>

<sup>1</sup>Microwave Photonics Research Laboratory, School of Electrical Engineering and Computer Science, University of Ottawa, Ottawa, Ontario K1N 6N5, Canada

<sup>2</sup>School of Physics Science and Technology, Nanjing Normal University, Nanjing 210023, China

\*Corresponding author: jpyao@eecs.uottawa.ca

Received 1 September 2015; revised 23 September 2015; accepted 24 September 2015; posted 24 September 2015 (Doc. ID 249080); published 21 October 2015

**An approach to the interrogation of a linearly chirped fiber Bragg grating (LCFBG) sensor using a linearly frequency-modulated (or chirped) optical waveform (LFMOW) with a high resolution is proposed and experimentally demonstrated. An LFMOW is generated at a laser diode through linear frequency modulation. The generated LFMOW is then launched into an LCFBG pair consisting of two identical LCFBGs, with one serving as a sensing LCFBG and the other as a reference LCFBG. The reflection of the LFMOW from the two LCFBGs would lead to two time delayed LFMOWs. By beating the LFMOWs at a photodetector, a microwave signal with a beat frequency that is proportional to the time delay difference between the two reflected LFMOWs is generated. By measuring the frequency change of the beat signal, the strain applied to the sensing LCFBG is estimated. The proposed approach is experimentally evaluated. An LCFBG sensor with a resolution of 0.25  $\mu\text{e}$  is experimentally demonstrated. © 2015 Optical Society of America**

**OCIS codes:** (060.3735) Fiber Bragg gratings; (140.3518) Lasers, frequency modulated; (060.2370) Fiber optics sensors.

<http://dx.doi.org/10.1364/OL.40.004923>

Fiber Bragg grating (FBG) sensors have been investigated extensively in the last few decades [1]. The operation of an FBG sensor is normally implemented by measuring the Bragg wavelength shift that is dependent on the measurand, such as strain or temperature [2]. To measure the Bragg wavelength shift, a number of interrogation schemes have been developed. For example, an optical edge filter can be used to perform high-speed interrogation of an FBG sensor by converting the wavelength shift to a light intensity change [3,4], but the interrogation resolution is usually poor. To increase the interrogation resolution, a tunable Fabry–Perot filter [5] or wavelength-swept fiber laser source [6] may be used, but the interrogation speed is limited, and may only be used for static or low-speed sensing.

For applications such as acoustic wave detection and vibration sensing, high interrogation speed, usually faster than 100 kHz, is needed [7,8]. In addition, the resolution of these methods is generally poorer than 1 pm [9]. For many applications, however, a higher resolution is required.

To increase the speed, interrogation of FBG sensors can be implemented based on microwave photonic (MWP) techniques to convert the wavelength shift in the optical domain to the amplitude or frequency change of a microwave signal in the electrical domain [10,11]. Since the amplitude or frequency of a microwave signal can be estimated at a high speed using a digital signal processing (DSP) unit [12], an MWP-based FBG sensor can provide ultra-fast sensing. For an MWP-based FBG sensor, if the Bragg wavelength shift is converted to the amplitude change of a microwave signal, the sensing resolution is still poor due to the optical power fluctuations in the system [13]. In addition, those systems normally have an interferometric structure that is sensitive to environmental disturbances [14]. Therefore, converting the Bragg wavelength shift to a frequency change of a microwave signal and then implementing frequency interrogation is a more reliable and robust solution with a better resolution. For example, in [15], the wavelength shift was converted to the microwave frequency change by incorporating the sensing FBG into an optoelectronic oscillator (OEO). When a strain is applied to the FBG, the Bragg wavelength is shifted, and the microwave frequency is accordingly changed. Since the interrogation is done by measuring the microwave frequency shift, the speed is fast and the resolution is high. The major limitation of the approach in [15] is that the system cannot be used for remote sensing since the OEO loop must be short and have a fixed length to ensure a stable operation with an accurate oscillation frequency.

In this Letter, we propose an approach to the interrogation of a linearly chirped fiber Bragg grating (LCFBG) sensor using a linearly frequency-modulated (or chirped) optical waveform (LFMOW) with a high resolution. In the proposed system, an LFMOW is generated at a laser diode (LD) through linear frequency modulation, which is done by injecting a sawtooth current into the LD. The generated LFMOW is then sent to an

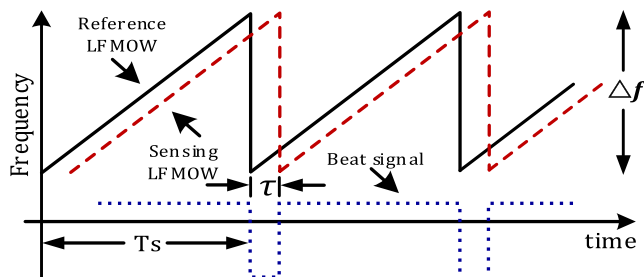
LCFBG pair consisting of two identical LCFBGs, with one serving as a sensing LCFBG and the other as a reference LCFBG. The reflection of the LFMOW from the two LCFBGs would lead to the generation of two time-delayed LFMOWs. By beating the LFMOWs at a photodetector (PD), a microwave beat signal with a frequency that is proportional to the time delay difference between the two reflected waveforms is generated. By measuring the frequency shift of the beat signal, the strain applied to the sensing LCFBG is estimated. The proposed approach is experimentally evaluated. An LCFBG sensor with a sensing resolution of  $0.25 \mu\epsilon$  is experimentally demonstrated. The key features of the proposed approach include high speed, high resolution, and high stability operation. In addition, the beat frequency is dependent only on the time delay difference between the two LCFBGs, and the absolute distance can be long, making the approach suitable for remote sensing.

Figure 1 illustrates the concept of the proposed approach. An LFMOW generated by an LD through linear frequency modulation is launched to an LCFBG pair consisting of a reference LCFBG and a sensing LCFBG. Because of the time delay difference between the two LCFBGs, two time-delayed LFMOWs are generated. The beating between the two time-delayed LFMOWs will generate a microwave waveform with its frequency proportional to the time delay difference. The linear frequency modulation at the LD is performed by direct modulation using a sawtooth injection current [16,17]. As shown in Fig. 1, the solid line represents the instantaneous frequency of the LFMOW reflected from the reference LCFBG, and the dashed line represents the instantaneous frequency of the LFMOW reflected from the sensing LCFBG with a time delay difference  $\tau$  caused by the distance between the two LCFBGs. The dotted line shows the beat frequency, which is dependent on the time delay difference. When a strain is applied to the sensing LCFBG, the spectral response of the sensing LCFBG is laterally shifted, which leads to the shift of the reflection point. The time delay difference is changed, which leads to the change of the beat frequency. By monitoring the beat frequency, the time delay is estimated, which is then used to calculate the Bragg wavelength shift and thus the strain.

In the following, we will derive the expression that shows the relationship between the strain applied to the sensing LCFBG and the beat frequency. For a reference LFMOW, the instantaneous optical frequency  $\omega_1(t)$  is given by

$$\omega_1(t) = \omega_0 + \alpha t, \quad (1)$$

where  $\omega_0$  is the angular frequency at the start of a period of the LFMOW, and  $\alpha$  is the frequency-modulation (chirp) rate that equals  $2\pi\Delta f/T_s$ , where  $\Delta f$  is the frequency deviation and  $T_s$



**Fig. 1.** Frequency relationship between the two time-delayed LFMOWs and the corresponding beat frequency.

is the period of the sawtooth waveform. The optical field of the reference LFMOW  $E_1(t)$  can be written as

$$E_1(t) = A_1 \exp \left[ j \left( \omega_0 t + \frac{1}{2} \alpha t^2 + \varphi_0 \right) \right], \quad (2)$$

where  $A_1$  is the amplitude and  $\varphi_0$  is the initial phase of the reference LFMOW. Similarly, the optical frequency and the optical field of the time-delayed sensing LFMOW can be written as

$$\omega_2(t, \tau) = \omega_0 + \alpha(t - \tau), \quad (3)$$

$$E_2(t) = A_2 \exp \left\{ j \left[ \omega_0(t - \tau) + \frac{1}{2} \alpha(t - \tau)^2 + \varphi_0 \right] \right\}, \quad (4)$$

where  $A_2$  is the amplitude of the sensing LFMOW, and  $\tau$  is the time delay difference between the two LFMOWs, given by

$$\tau = 2nL/c, \quad (5)$$

where  $L$  is the distance between the two LCFBGs,  $n$  is the refractive index of the fiber, and  $c$  is the velocity of light in vacuum. When these two waveforms are applied to a high-speed PD, a beat signal is generated, given by [18]

$$i(t, \tau) = R |E_1(t) + E_2(t, \tau)|^2 = R \left[ I_1 + I_2 + 2\sqrt{I_1 I_2} \cos \left( \alpha \tau t + \omega_0 \tau - \frac{1}{2} \alpha \tau^2 \right) \right], \quad (6)$$

where  $I_1$  and  $I_2$  are the intensities of the reference and sensing signals, respectively, and  $R$  is the responsivity of the PD. From Eq. (6), we have the frequency of the beat signal  $f_b$ , given by

$$f_b = \frac{\alpha \tau}{2\pi}. \quad (7)$$

According to Eq. (7), the time delay difference  $\tau$  caused by the distance between the two LCFBGs and the frequency-modulation rate  $\alpha$  are the two parameters that determine the fundamental beat frequency. For a given sensing range, the distance should be selected short to make the two LCFBGs locate closely, which would reduce the impact of the environmental temperature change on the relative distance between the LCFBGs, making the sensor more stable for strain sensing.

It is known that the Bragg wavelength shift for a strain applied to an LCFBG can be expressed as [1]

$$\Delta\lambda = \lambda_0(1 - P_e)\Delta\epsilon, \quad (8)$$

where  $\Delta\lambda$  is the wavelength shift induced by the strain,  $P_e$  is the effective strain-optic coefficient and has a numerical value of 0.22 at 1550 nm,  $\lambda_0$  is the initial wavelength at a specific reflection point in the LCFBG, and  $\Delta\epsilon$  is the applied strain.

For an LCFBG with a chirp rate  $C_{\text{chirp}}$  (nm/cm), by using Eq. (8), we have the relationship between the strain-induced time delay  $\Delta\tau$  and the applied strain,

$$\Delta\tau = \frac{2n\lambda_0}{cC_{\text{chirp}}}(1 - P_e)\Delta\epsilon, \quad (9)$$

and the relationship between the beat frequency shift and the applied strain is given by

$$\Delta f_b = \frac{\alpha}{2\pi} \times \frac{2n\lambda_0}{cC_{\text{chirp}}}(1 - P_e)\Delta\epsilon. \quad (10)$$

By measuring the frequency shift of the beat signal caused by the variation of the time delay, the strain could be determined.

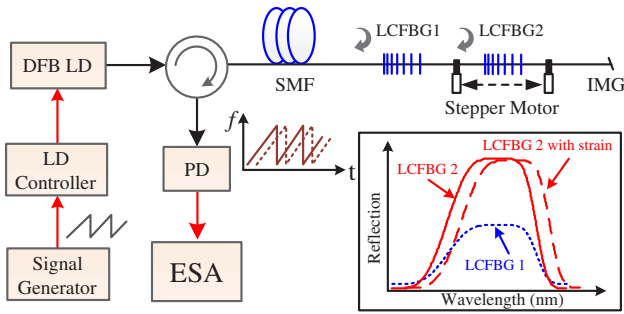


**Fig. 2.** Experimental setup. Inset: the spectrum of the reference LCFBG (LCFBG1) and the spectra of the sensing LCFBG (LCFBG2) when two different strains are applied.

The proposed approach is experimentally evaluated. Figure 2 shows the experimental setup. A distributed feedback (DFB) LD operating at 1546.3 nm is directly modulated by a sawtooth injection current, which is generated by an LD controller (ILX Lightwave LDC-3722) driven by a sawtooth wave generated by a function generator (Agilent 33250A). The sawtooth injection current has a repetition rate of 1 MHz with a peak-to-peak current of 40 mA on a DC bias current of 180 mA, providing a linear frequency modulation over a frequency range of 20 GHz. An LFMOW is thus generated that is then launched into the LCFBG pair consisting of a reference LCFBG (LCFBG1) and a sensing LCFBG (LCFBG2). The two LCFBGs are fabricated by UV exposure using a linearly chirped phase mask. Their resonance wavelengths are centered at 1547.3 nm with a reflection bandwidth of 4 nm. Both LCFBGs have the same physical length of 1.7 cm and the same dispersion of 19.8 ps/nm. The chirp rate for both LCFBGs is 2.432 nm/cm. The distance between the two LCFBGs is 1.5 cm.

It is obvious that the LCFBG pair forms a Fabry–Perot cavity. To make the powers of the two reflected light waves identical and to decrease the effects of multiple reflections in the cavity, the reflectivities are chosen to be around 30% and 70% for LCFBG1 and LCFBG2, respectively, by controlling the UV exposure time during the fabrication process. The spectra of the two LCFBGs are shown in the inset in Fig. 2. The reflected LFMOWs are then sent to a PD through an optical circulator. The generated microwave signal at the output of the PD is sent to an electrical spectrum analyzer (ESA, Agilent E4448A).

To have small sensing error, the LCFBGs should be designed and fabricated with small ripples. Figure 3 shows the measured reflection magnitude response and the group delay response of the sensing LCFBG (LCFBG2). As can be seen, the group delay response is smooth with small ripples, which is

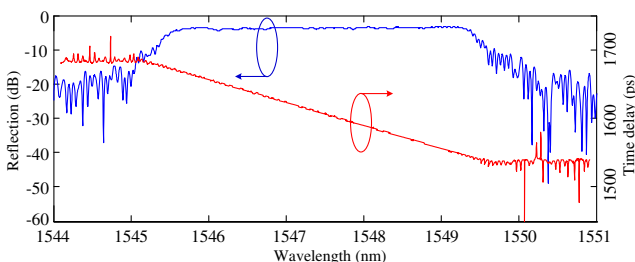


**Fig. 3.** Measured reflection spectrum and time delay response of the sensing LCFBG.

achieved by applying a Gaussian apodization profile to the LCFBG during the fabrication. Since the ripples are small, high-precision sensing is ensured. In the experiment, LCFBG2 is mounted on an actuated stage, and the strain is applied by a stepper motor. When a strain is applied to LCFBG2, the beat frequency is shifted. Figure 4 shows the measured frequency as a function of the applied strain. In the experiment, the beat frequency is measured by the ESA. As can be seen in Fig. 4, when the strain is increased, the beat frequency of the generated beat signal is increased. The spectrum of the beat signal is shown in the inset of Fig. 4. When a strain is increased from 30 to 300  $\mu\epsilon$ , the frequency of the generated beat signal is shifted from about 853 to 996 KHz. The results in Fig. 4 confirm the expected linear relationship between the applied strain and the frequency of the generated beat signal, as predicted by Eq. (10). The sensitivity is estimated by linearly fitting the measurements in Fig. 4, which is 0.483 KHz/ $\mu\epsilon$ . Again, the result agrees well with the theoretical value of 0.475 KHz/ $\mu\epsilon$  that can be calculated using Eq. (10). Considering the frequency measurement resolution limit ( $\sim 0.1$  KHz) of the ESA, the sensing resolution is estimated to be 0.25  $\mu\epsilon$ .

It should be noted that, due to the multiple reflections between the two LCFBGs, at the output of the PD, we may have beat signals with beat frequencies that are multiple times the fundamental beat frequency. Figure 5 shows the spectrum of

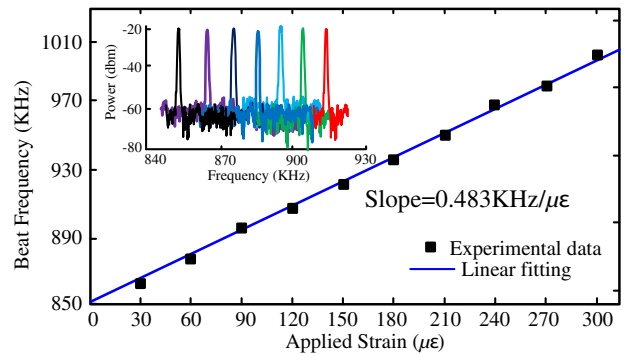


**Fig. 4.** Measured beat frequency as a function of the applied strain. Inset: the measured electrical spectrum of the beat signal for different strains.

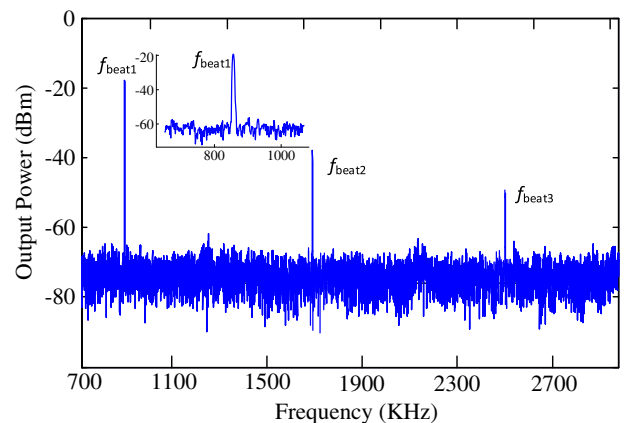


**Fig. 5.** Electrical spectrum of the first three beat signals. Inset: the zoom-in view of  $f_{beat1}$ .

the electrical signal at the output of the PD with no strain applied. As can be seen, multiple beat signals at 0.853, 1.706, and 2.559 MHz are generated.

In our experiment, the fundamental beat signal with the highest power is chosen as the frequency to be measured since it offers the best signal-to-noise ratio. However, to avoid measurement ambiguity, the frequency range is limited, which is the fundamental beat frequency. In the experiment, the fundamental beat frequency is 853 KHz. Considering the sensing sensitivity is 0.475 KHz/ $\mu\epsilon$ , the maximum strain that the interrogator can measure is 1796  $\mu\epsilon$ . This value is high enough for most applications. In addition, by increasing the distance between the two LCFBGs, a higher fundamental beat frequency will result, which will increase the measurement range.

Temperature change has negligible impact on the strain measurement because the two LCFBGs have relatively short lengths and are placed in close proximity. The change of environmental temperature will lead to an identical change to the wavelengths of the two LCFBGs; thus, the relative distance between the two LCFBGs is maintained unchanged, making the beat frequency independent of the environmental temperature change. To experimentally evaluate the dependence of the sensor on the environmental temperature change, we place the sensing LCFBG (without strain) and the reference LCFBG in a temperature-controlled oven. The temperature is increased from 20°C to 60°C, and the fundamental beat frequency is monitored. The results show that the fundamental frequency is maintained unchanged.

The resolution of the proposed sensor system can be adjusted in two ways: by adjusting the dispersion of the LCFBGs or by adjusting the chirp rate of the LFMOW. In the first approach, if the dispersion of the LCFBGs is increased, for a given beat frequency shift, a smaller time delay is needed. Thus, a smaller strain will cause a greater beat frequency shift, leading to an increased resolution. For example, if the dispersion of the LCFBGs is increased from 19.8 ps/nm to 1000 ps/nm, the resolution will be increased about 50 times. A simple method to achieve an adjustable resolution is to increase the frequency modulation (chirp) rate of the generated LFMOW, which can be done by simply increasing the slope of the sawtooth waveform from the function generator. However, there is a trade-off between the resolution and measurement range if the second approach is employed. In addition, the use of a sawtooth injection current will also introduce intensity modulation to the generated LFMOW, which may cause an error to the frequency measurement.

The interrogation speed of the proposed sensing system is decided by the scanning rate (typically several KHz) of the ESA. For practical applications, a DSP unit may be used to measure the frequency, and the interrogation speed can be greatly improved, which would make the proposed approach suitable for high-speed dynamic sensing with small size.

In conclusion, we have proposed and experimentally demonstrated an approach to the interrogation of an LCFBG sensor based on the LFMOW with high resolution. The fundamental

principle of the approach is to translate the Bragg wavelength shift of the sensing LCFBG to the frequency shift of the beat signal generated by beating two time-delayed LFMOWs reflected from the sensing and reference LCFBGs. By measuring the beat frequency, the strain applied to the sensing LCFBG could be measured. The proposed approach was experimentally evaluated. By using two identical LCFBGs separated by 1.5 cm, with each having a physical length of 1.7 cm and a value of dispersion of 19.8 ps/nm, a strain sensor with a resolution of 0.25  $\mu\epsilon$  was demonstrated. The key features of the proposed approach include high speed, high resolution, and high stability operation. In addition, the beat frequency is dependent only on the time delay difference between the two LCFBGs. The absolute distance can be an arbitrary wave, and thus it is suitable for remote sensing.

**Funding.** National Natural Science Foundation of China (NSFC) (61307108); Natural Sciences and Engineering Research Council of Canada (NSERC).

Y. Wang acknowledges support from the Jiangsu Overseas Research & Training Program.

## REFERENCES

1. A. D. Kersey, M. A. Davis, H. J. Patrick, M. LeBlane, K. P. Koo, C. G. Askins, M. A. Putnam, and E. J. Friebele, *J. Lightwave Technol.* **15**, 1442 (1997).
2. Y. Wang, Y. Cui, and B. Yun, *IEEE Photon. Technol. Lett.* **18**, 1539 (2006).
3. S. M. Melle, K. Liu, and R. M. Measures, *IEEE Photon. Technol. Lett.* **4**, 516 (1992).
4. M. Song, S. Yin, and P. B. Ruffin, *Appl. Opt.* **39**, 1106 (2000).
5. A. D. Kersey, T. A. Berkoff, and W. W. Morey, *Opt. Lett.* **18**, 1370 (1993).
6. S. H. Yun, D. J. Richardson, and B. Y. Kim, *Opt. Lett.* **23**, 843 (1998).
7. H. Fu, W. Zhang, C. Mou, X. Shu, L. Zhang, S. He, and I. Bennion, *IEEE Photon. Technol. Lett.* **21**, 1078 (2009).
8. H. J. Bang, S. M. Jun, and C. G. Kim, *Meas. Sci. Technol.* **16**, 813 (2005).
9. Y. Rao, *Meas. Sci. Technol.* **8**, 355 (1997).
10. X. Dong, L. Y. Shao, H. Fu, H. Tam, and C. Lu, *Opt. Lett.* **33**, 482 (2008).
11. L. Shao, X. Dong, A. Zhang, H. Y. Tam, and S. He, *IEEE Photon. Technol. Lett.* **19**, 30 (2007).
12. P. Asbeck, I. Galton, K. C. Wang, J. F. Jensen, A. K. Oki, and C. T. M. Chang, *IEEE Trans. Microwave Theory Tech.* **50**, 900 (2002).
13. T. Wei, J. Huang, X. Lan, Q. Han, and H. Xiao, *Opt. Lett.* **37**, 647 (2012).
14. R. Cheng, X. Li, J. Yan, J. Zhou, Y. Wen, and J. Rohollahnejad, *IEEE Photon. Technol. Lett.* **27**, 1577 (2015).
15. F. Kong, W. Li, and J. P. Yao, *Opt. Lett.* **38**, 2611 (2013).
16. P. K. C. Chan, W. Jin, J. M. Gong, and M. S. Demokan, *IEEE Photon. Technol. Lett.* **11**, 1470 (1999).
17. S. Gao and R. Hui, *Opt. Lett.* **37**, 482 (2012).
18. J. Zheng, *Appl. Opt.* **43**, 4189 (2004).